# Supporting Information

The Effect of Ultraviolet Radiation on Organic

Photovoltaic Materials and Devices

Jay B. Patel [1], Priti Tiwana[2], Nico Seidler[2], Graham E. Morse[2], Owen R. Lozman[2], Michael B. Johnston[1] , and Laura M. Herz[1]*

1. Department of Physics, Clarendon Laboratory, University of Oxford, Parks Road, Oxford, OX1 3PU, United Kingdom

E-mail: laura.herz@physics.ox.ac.uk

2. Merck Chemicals Ltd., Chilworth Technical Centre, University Parkway, Southampton, SO16 7QD, United Kingdom
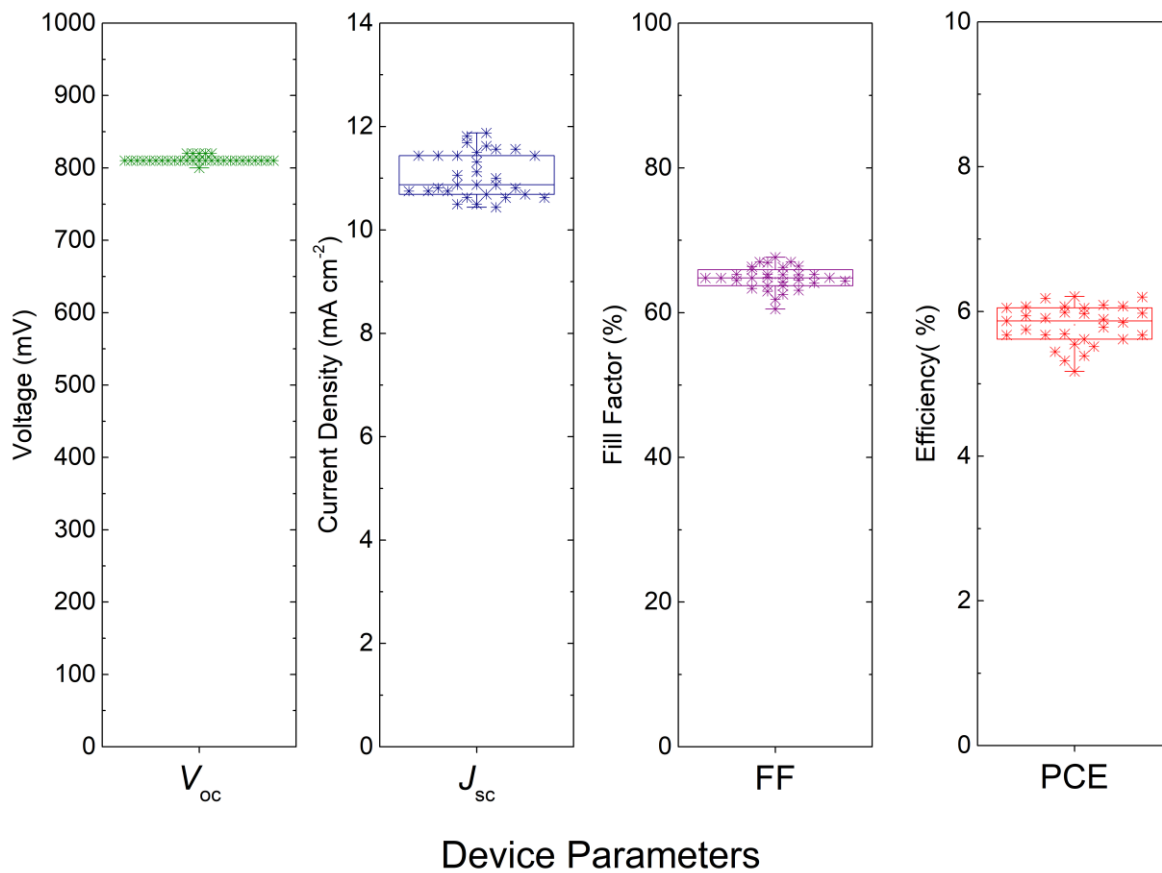
Figure S1. Device parameters found using standard *JV* characterisation, for the device batch used in this study, with the open-circuit voltage (V_{oc}), short-circuit density (J_{sc}), fill factor (FF) and power conversion efficiency (PCE). The devices were measured promptly after fabrication. These devices were then used for the investigation.
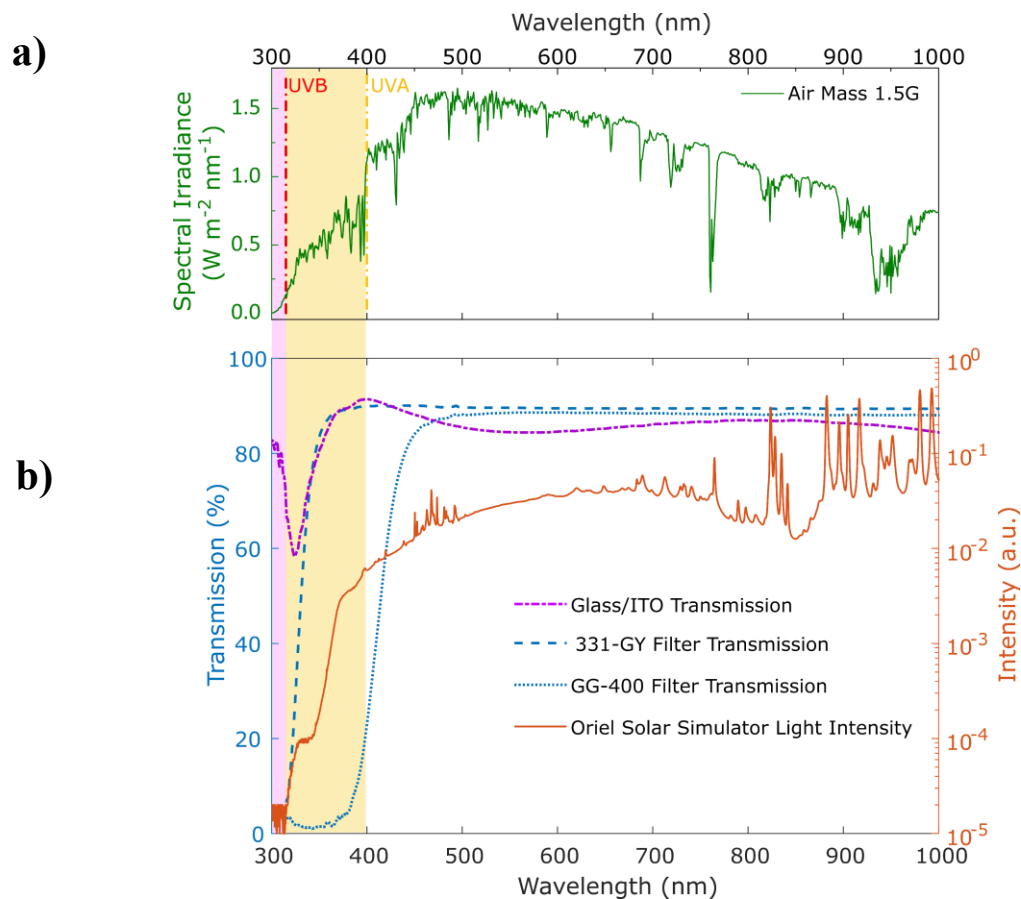
Figure S2. a) Air Mass 1.5G solar spectrum, plotted using data accessed from nrel.gov.[1] The dashed lines denote the cut-off for the two categories of UV radiation found in the AM 1.5 solar spectrum, UVB ($280 \leq \lambda < 315$ nm) and UVA ($315 \leq \lambda < 400$ nm) **b)** The transmission spectrum of the long pass 331nm filter (H-BaK7 331-GY, Comar optics) used in this investigation to filter UVB radiation, and the transmission spectrum of the long pass 400 nm filter (Schott Glass GG-400, Thorlabs) that was used to filter UVB +UVA radiation, together with the simulated unfiltered AM 1.5 light spectrum (red line) generated from the Oriel class AAA solar simulator with 0.7 sun (70mWcm^{-2}) intensity. The pink line shows the transmission curve of the glass/ITO substrates that the devices were fabricated on. The glass/ITO reflects a fraction of the incident light across the whole frequency range, and clearly transmits a significant amount of UV radiation.
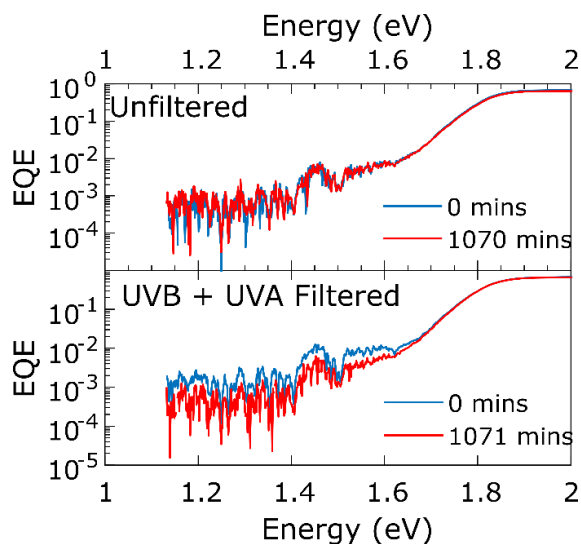
Figure S3. Sub-bandgap changes in the EQE, as evident when spectra shown in Figure 1c are plotted on a semi-logarithmic scale. A reduction in photocurrent from the sub-bandgap region is evident when the device is exposed to UVB+UVA filtered AM1.5 light (bottom), while no change is found when the device is exposed to unfiltered AM1.5 light (top).
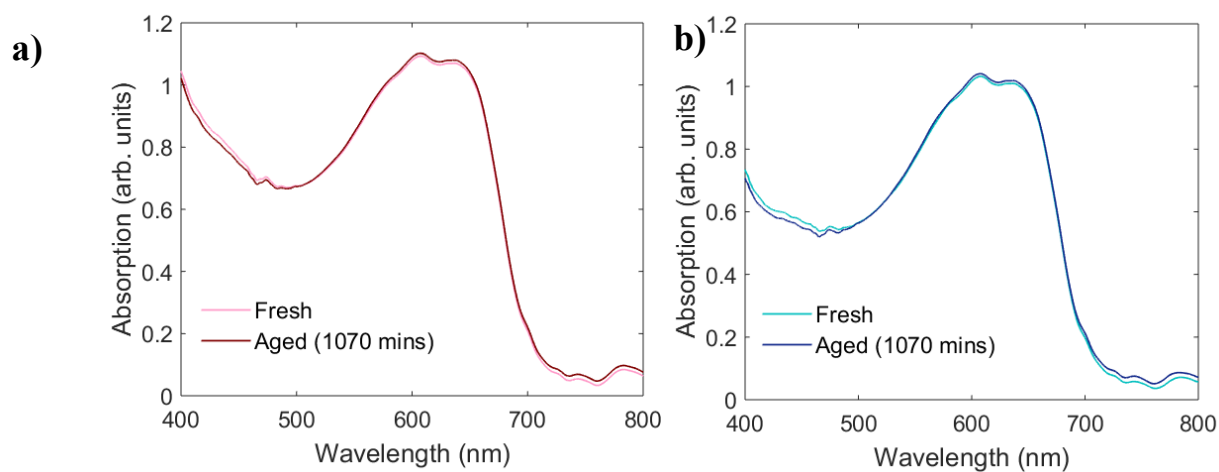

Figure S4. Ultraviolet-visible absorption spectra of the bulk heterojunction films containing PBTZT-stat-BDTT-8 and PCBM when illuminated with **a)** unfiltered **b)** UVB + UVA filtered AM 1.5 light before (fresh) and after 1070 mins (Aged).
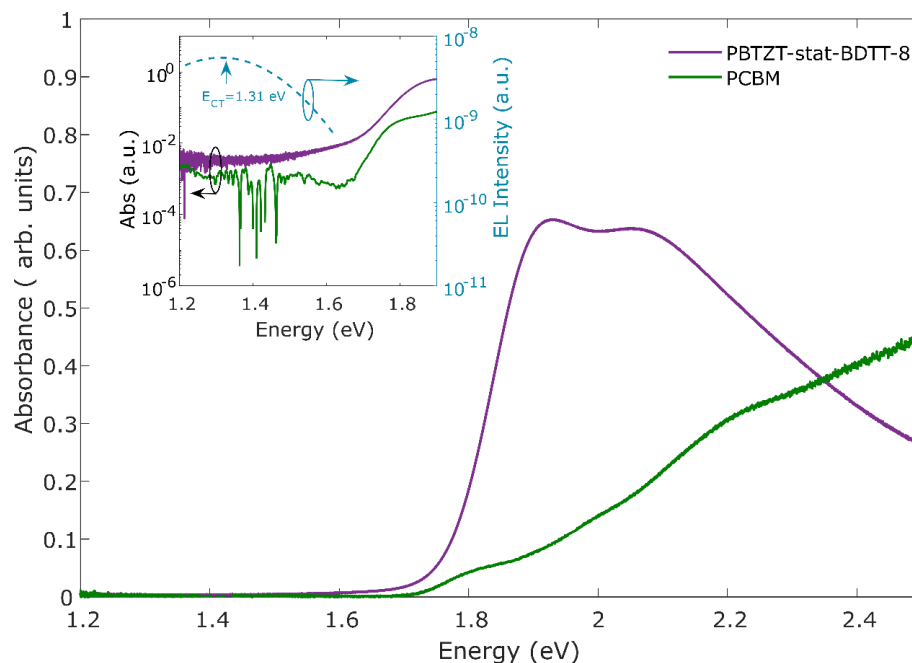
Figure S5: Absorption spectra of PBTZT-stat-BDTT-8 and PCBM on Quartz. The inset shows the sub-bandgap absorbance of PBTZT-stat-BDTT-8 and PCBM along with the recorded electroluminescence spectra of the fresh device. The arrows represent the y-axis that the data corresponds to.
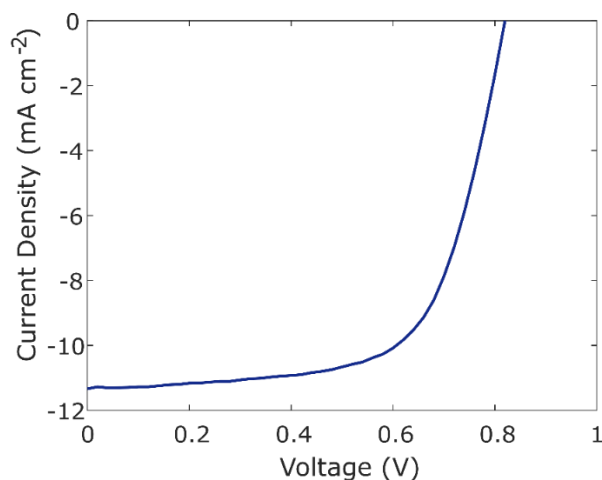
Figure S6: Current-voltage curve of a typical PBTZT-stat-BDTT-8:PCBM bulk heterojunction device.
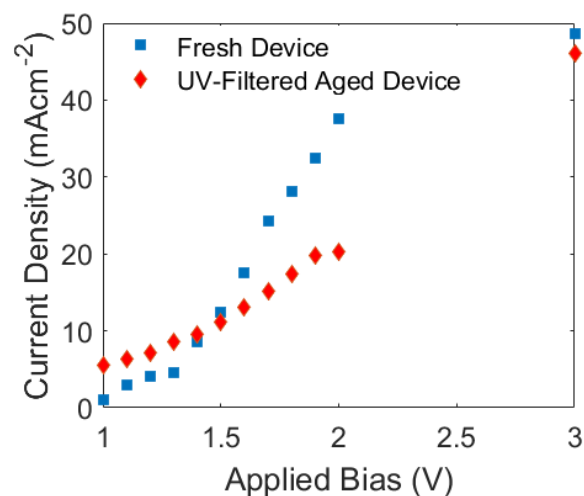
Figure S7: Bias voltage applied to the OPV device and the corresponding injection current density measured during electroluminescence spectroscopy. To extract an accurate value of E_{CT} it is important to ensure that EL spectra are measured in the low injection current regime (<30 mA cm^{-2}), as this minimizes local changes in the chemical potential of the PAL.[2] From Figure S7 it is clear that the plateauing observed in Figure 3c after 1.6 V is below the low injection regime, allowing us to extract an accurate value of E_{CT}= 1.31eV.

Illumination Condition	Initial (mA cm^{-2})	Aged (mA cm^{-2})
Unfiltered Light	13.05	12.29
UVA +UVB Filtered Light	12.19	11.56

Table S1: The absolute integrated short-circuit current density values of the initial and aged devices (1070 minutes) from Figure 2.

References

[1]   NREL. NREL National Center for Photovoltaics http://www.nrel.gov/ncpv/ (accessed March 19, 2017).

[2]   Vandewal, K.; Albrecht, S.; Hoke, E. T.; Graham, K. R.; Widmer, J.; Douglas, J. D.; Schubert, M.; Mateker, W. R.; Bloking, J. T.; Burkhard, G. F.; et al. Efficient Charge Generation by Relaxed Charge-Transfer States at Organic Interfaces. Nat. Mater. 2014, 13 (1), 63–68.